Analysis of *M. oryzae* Cdc14 phosphatase reveals potential inhibitor as candidate for broad-spectrum fungicide

Kaitlyn D. Crowley, Hyowon (Raphi) Kang, Alan D. Tondryk
Summer Science Program in Biochemistry at Purdue, July 2018

Abstract

Rice Blast disease, responsible for up to 30% of global rice loss each year, is caused by the fungus *Magnaporthe oryzae*. The tyrosine phosphatase Cdc14 is a critical functional component that is conserved across many organisms, including *M. oryzae*, but is not present in plants. Cdc14 homologs in other organisms play important functions for survival. For example, the budding yeast Cdc14 homolog plays an important role in cell replication. In addition, deletion of Cdc14 in *Aspergillus flavus*, a pathogen similar to *M. oryzae* that infects plants, results in defective growth of the fungus population. Therefore, we hypothesized that creating an inhibitor of Cdc14 will inhibit growth of the *M. oryzae* population. In our lab, we produced, purified, and characterized our enzyme for study. We then tested the affinity of different substrates for M.O. Cdc14. Our results suggest that the binding site of our enzyme retains conserved Cdc14 specificity. Testing of different inhibitors revealed that benserazide (inhibitor I2) is an effective irreversible inhibitor of M.O. Cdc14, and can thus serve as a potential pesticide component. We have discovered that a further modified structure of I2 created *in silico* expresses much greater affinity for the binding site.

Introduction

As the world population grows to unprecedented numbers, the need for efficiency in nutriment production is at its maximum. In 2016, approximately 11% of the world's population was affected by food insecurity[1]. However, every year crops all over the world are rendered inedible due to fungal epidemics. One notable fungus is *Magnaporthe oryzae*, which mainly affects rice but can also affect wheat and barley. Rice blast disease, caused by *M. oryzae*, is the source of up to 30% of global rice loss each year[2]. Presently available fungicides can be harmful to the environment and have low effectiveness, as *M. oryzae* can develop resistance to genetic changes in plants and current fungicides in relatively few growing cycles[3]. Hence the work of inhibiting such fungi is meaningful to our society.

One possible way to control the pathogen is to inhibit its Cdc14 enzyme, a phosphatase. The coding sequence for Cdc14 is a highly conserved area of many fungi, including *M. oryzae*, and has been shown to play crucial parts in the function and survival of other organisms[4]. In budding yeast, Cdc14 counteracts CDK phosphorylation and inactivates its function, thereby enabling mitotic exit[5,6]. Mitotic exit is the concluding step of mitosis, where the cell must reorganize from its mitotic state to its interphase state. Budding yeast with mutated Cdc14 have been shown to cease replication[7]. Mutation of Cdc14 in a similar fungus, *Aspergillus flavus*, also adversely affects cell development[8]. Since the Cdc14 in *M. oryzae*, a similar fungus, plays a crucial role in fungal development, we can hypothesize that inhibiting the Cdc14 will deprive the fungus of its ability to replicate and sustain its population.

Cdc14 is a good target for inhibition for several reasons. It is a gene that is highly conserved and has an important function that, when inhibited, will deter the livelihood of the fungus. The fact that Cdc14 is such a highly conserved site means that the creation of an inhibitor for *M. oryzae* Cdc14 has the potential to act as a broad fungicide. At the same time, the lack of Cdc14 genes in plants suggests that our Cdc14 inhibitor will not disturb plant growth. Cdc14 also has a specific binding site with known location and properties, so it is a convenient site to inhibit[9]. It is further made a good target as its previously studied kinetic properties and similar models constructed via X-ray crystallography suggest that the active site recognizes specific, mimickable structures.[10].

Thus, we sought to characterize MoCdc14 and design an effective inhibitor of *M. oryzae* Cdc14. In this paper, we will discuss our work of characterizing and designing a potential inhibitor for this protein, which can be produced and synthesized in the future for testing and possible real life implementation. Designing an inhibitor to target *M. oryzae* Cdc14 will be the

first step in the development process of a chemical fungicide to target fungal crop pathogens.

Results & Discussion

Bioinformatics

To begin the project, it was important to ascertain that our given sequence of M.O. Cdc14 was indeed that of M.O. Cdc14, so we performed a blast search with the sequence. The most identical homologs identified by the search, with ~100% identity and ~0.0 E-values, were all M.O. Cdc14 phosphatases, which established the fact that we were working with the correct sequence. In Jalview, we then aligned our sequence with that of homologs found in the blast search. The conservation of the active site components amongst the sequences present, our enzyme included, allowed us to conclude that our enzyme must indeed be *M. oryzae* Cdc14 (Fig. 1A).

Bacterial transformation

With the ultimate goal of inhibiting *M. oryzae* Cdc14, we cultured *E. coli* transformed with a pGEX-6P-1 plasmid encoding the *M. oryzae* homolog of Cdc14, a His-tag, and ampicillin resistance. Survival of bacterial colonies on a plate treated with ampicillin indicated successful bacterial transformation. To confirm that our protein was induced, we performed SDS-Page gel electrophoresis with the induced and uninduced sample. Analysis of the gel in Image Lab (Fig. 2A) showed that a band in the induced lane was amplified, further indicating induction of the bacterial cells. This band, our target protein, was located between the 66.2 and 45 KDa bands in the molecular weight marker lane. Thus, we could observe that our target protein had a molecular weight between 45 and 66.2 KDa, which corroborated our Expasy result of 53.5 KDa.

Protein purification and analysis

The Cdc14 enzyme was overexpressed in our E. coli (Fig. 2A) cultures and purified by Ni-NTA chromatography (Fig. 2B). Analysis of the gel in imageLab showed that the protein had been successfully purified and that it had an average molecular weight of 54.4 kDa. The calculated molecular weight of 54.4 KDa corroborated the molecular weight of 53.5 KDa obtained by Expasy, with a 2.0% difference. The absence of additional significant bands signified successful purification. Faint bands in the purified Cdc14 lane near the 35 and 25 KDa marks were the result of extraneous cutting by the cellular proteases. We confirmed the identity of the protein by peptide mass fingerprinting, where this result had a $10^{-12.6}$ chance of being random.

Assays to Determine Specific Activity

Because we had initially transformed our bacteria with a plasmid encoding Cdc14, a tyrosine phosphatase, we hypothesized that our enzyme would be a tyrosine phosphatase. We determined the specific activity of our enzyme, using pNPP (p-Nitrophenyl Phosphate) as the substrate in the presence and absence of the inhibitor sodium orthovanadate. pNPP contains a phosphate group and yields pNP if dephosphorylated, and sodium orthovanadate is a competitive inhibitor for tyrosine phosphatases. We calculated our average specific activity values to be 5.96 ± 0.01 min^{-1} in the absence of sodium orthovanadate, and 4.01 ± 0.37 min^{-1} in its presence (Fig. 1B). The presence of any activity with pNPP as substrate allowed us to conclude that our enzyme was indeed a phosphatase, and the decrease in activity when inhibited correlated with an expected decrease that a phosphatase inhibitor would cause. However, the high activity even in the presence of inhibitor suggested that while our protein was a phosphatase, it was unlikely to be a tyrosine phosphatase. It should be noted that the calculated specific activity may be affected by absorbance values close to 1. Thus, we cannot be certain that linearity was maintained while data was collected.

Enzyme Characterization

To further characterize our enzyme in order to design an effective inhibitor molecule,

we ran an assay with our enzyme at differing pNPP concentrations, under steady state conditions, to obtain the V_{max}, k_{cat}, and K_m values of our enzyme with pNPP. We determined that *M. oryzae* Cdc14's K_m was 9.12 ± 2.26 mM (Fig. 3). These values helped us determine the substrate concentrations in which we ran further assays. With the characterization completed, we could begin to empirically analyze the specificities of our enzyme's binding site.

Substrate Specificity

We hypothesized that *M. oryzae* Cdc14 would have the same binding site specificity as that of its Cdc14 homologs, as its active site sequence was highly conserved when compared to other Cdc14 sequences. Given that Cdc14 prefers substrates with a phosphorylated serine, a +3 lysine residue, and one or more basic residues next to that lysine [10], we predicted that substrate 24 would have the highest affinity for our enzyme due to its phosphorylated serine residue, lysines in the +2 and +3 position, and arginine at the +4 position (Fig. 4A). To test this hypothesis, we estimated k_{cat}/K_m by measuring activity at a single concentration of substrate. We saw that substrate 24 indeed had the greatest catalytic efficiency with our enzyme (Fig. 4B), s followed by substrates 21 and 7, whose phosphorylated serine and two K residues on and next to the +3 site also complement the conserved Cdc14 active site sequence. Thus, *M. oryzae* Cdc14 retains the previously observed yeast Cdc14 binding site specificity (ref). This corroborated our hypothesis that an inhibitor designed for *M. oryzae* Cdc14 would have broad function against other pathogens in the same family.

Enzyme Modelling & Inhibitor Affinity *in silico*

We then wanted to find an inhibitor with a high beginning affinity for our enzyme that we could further modify in the future. With the binding site analyzed based on its performance with different substrates, we began to test the affinity between our enzyme and existing inhibitors(Fig. 5A). First, to test inhibitor affinity *in silico*, *M. oryzae* Cdc14 was modeled by comparison with a yeast homolog in the MOE software. The most important part for our purposes, the active site, was conserved across both proteins. There were some sites that were not conserved between the M.O. Cdc14 homology model and the yeast homolog (Fig. 5B), but they did not alter the active site structure. This allowed us to test 16 different inhibitors docked in our homology model protein active site.

Inhibitor Affinity *in vitro*

To build on previous data gathered in silico and find the best inhibitor out of this set, we tested the 16 inhibitors *in vitro*. The *in silico* results did not correlate with the results from *in vitro* inhibitor testing possibly because we did not use an actual crystal structure, rather a homology model in MOE (Fig. 5C, Table 1). The experimentally determined percent inhibition from one trial showed G7, G6, I1, and G5 to be the most effective inhibitors. This is substantially varied from the MOE predictions, where I1, E1, and D7 were predicted to be the most effective.We decided to weigh the *in vitro* results more heavily than the *in silico* results in determining which three inhibitors we would further characterize with an IC_{50} assay. Accounting for shortage of supply, we assessed inhibitors I1, I2, and G5. IC_{50} values were determined for each inhibitor. We were able to get IC_{50} values of 8.68, 31.9, and 13.6 μM for I1, I2, and G5 respectively. I2 had the greatest IC_{50} value at 31.9μM (Fig. 6A). We further studied the mechanism of inhibition for inhibitor I2 (I1 and G5 were not used due to short supply).

I2 Binding Mechanism

We wanted to test the binding mechanism of I2 to so that we could better modify it for greater affinity in the future. We used a time sensitive assay to determine whether it bound to the active site of our enzyme reversibly or irreversibly. We discovered that the longer we preincubated the enzyme and inhibitor in solution before initiating reaction with pNPP,

the greater our percent inhibition (Fig. 6B). Since percent inhibition was dependent on the preincubation time, we concluded that I2 binds irreversibly to the active site of the enzyme. Note that in Figure 6 B, Trial 1 lacks a data point with a 60 minute preincubation time because the reaction was stopped prematurely during experimentation.

Designing Greater Affinity Inhibition

With the binding mechanism of I2 determined, we began to maximize the specificity and binding affinity of I2 towards our protein via structural modification in MOE. I2 started with a predicted binding affinity of -7.66 kal/mol; after modifications, the new compound had a predicted binding affinity of -16.54 Kcal/mol (Fig. 7A). Our new molecule was also able to take advantage of a hydrophobic pocket near the active site that the original I2 molecule simply could not reach. These modifications allowed for greater intermolecular forces, resulting in a greater binding affinity, which in turn allowed for greater specificity (Fig. 7B, 7C).

Conclusion

In this study, we have purified and characterized *M. oryzae* Cdc14. We verified that our enzyme was a phosphatase, and that its active site retained the conserved Cdc14 specificity. We then tested a collection of inhibitors with our enzyme to select I2 and further characterize its binding mechanism with our enzyme, before modifying it to make an inhibitor with greater binding affinity for *M. oryzae* Cdc14. Our findings suggest that *M. oryzae* Cdc14 can be effectively inhibited with the modified I2 inhibitor structure. With this inhibitor structure designed, the next step in this project will be further *in vitro* testing with *M. oryzae* Cdc14 and a synthesized version of our designed molecule. We can then test the synthesized inhibitor with Cdc14 from other pathogenic fungi, as the ultimate goal of the project is to create a chemical fungicide that can have broad application for fungal pathogens.

Methods

Bacterial transformation

E. coli transformed with plasmids encoding Mo Cdc14 with a His-tag and ampicillin resistance were used to produce the target protein Cdc14 found in the fungi *Magnaporthe oryzae*. Two sets of similar E. coli were grown in 2xYT media (5g/L NaCl, 16 g/L tryptone in water, 5g/L yeast extract) and then plated onto two plates containing ampicillin. Two samples of the surviving colonies, one later induced to produce Cdc 14 using L-arabinose, were cultured in 1 L of 2xYT media. Lysis buffer, Leupeptin, Pepstatin, and universal nuclease were added to break up the cells once we had enough bacteria. The supernatant, containing our protein, was filtered out using centrifugation and later used in the AKTA purification system. 20µL of uninduced and induced samples, along with 5µL of the molecular weight standard, were loaded into and run through a SDS-PAGE stacking and resolving gel for one hour at a voltage of 180V. The gel was submerged in fixing solution (25% isopropanol and 10% acetic acid in water) for 20 minutes, Coomassie blue staining solution (10% acetic acid, and 0.01% Coomassie brilliant blue in water) for at least 4 hours, and destain solution (10% acetic acid in water) for the night afterwards.

Protein purification and analysis

Cell pellet supernatant from centrifugation was loaded and run through the AKTA system, using Nickel Buffer A (25 mM HEPES pH 7.5, 500 mM NaCl, 10% glycerol in water) and B (25 mM HEPES pH 7.5, 500 mM NaCl, 250 mM imidazole, 10% glycerol in water).The protein was collected on the Nickel column while using buffer A then washed off and collected using buffer b. The resulting protein extract was collected in thirty microfuge tubes. Overnight dialysis in storage buffer (25 mM HEPES pH 7.5, 300mM NaCL, 2mM EDTA, 0.1% 2-mercaptoethanol, 40% v/v glycerol) was performed on the pooled samples from microfuge tubes that corresponded with the

highest protein concentration in the purification graph. 1 mL of the dialysis result was aliquoted into each of 17 microfuge tubes for future use. A Bradford assay was performed to determine the concentration of the protein solution and gel electrophoresis was conducted on a sample of the pooled protein solution.

Assays to Determine Specific Activity

To determine the specific activity of our enzyme, we ran an assay in triplicate with two 400 µL samples of 1 µM enzyme in reaction buffer (25 mM Hepes pH 7.5, 0.1% 2-mercaptoethanol, 1 mM EDTA, 150 mM NaCl). One reaction was run with 50mM sodium orthovanadate inhibitor, and another without. 50µL of 5N NaOH was used to quench the reactions after 15 minutes in the incubator at 30 C^o The concentration of the product produced, pNP (p-Nitrophenyl), was calculated using the absorbance from analysis in a SpectroVis at 405.4 nm and a known extinction coefficient of pNPP (p-Nitrophenyl Phosphate) as in Equation 1.

Equation 1

$$A = \varepsilon CI$$

Given the concentration of pNP, we calculated the specific activity of our enzyme.

Enzyme Characterization

The protein sequence for Cdc14 in *M. oryzae* was compared with Human and yeast orthologs found in a protein blast search by aligning their sequences in Jalview. To further characterize our enzyme, we established steady state conditions by adding different concentrations of enzyme to 100 mM pNPP reaction buffer and allowing for the reaction to progress. Then we performed linear regression with our data on Logger Pro to determine the enzyme concentration at which the absorbance vs. time plot remained linear for 15 minutes. This was done to determine an optimal enzyme concentration for our steady state conditions to run further reactions. A standard curve was generated based on an assay using pNP solutions of 5 µM to 100 µM, with the absorbances measured using a SpectroVis at 405.4 nm. We ran another assay to determine optimum substrate concentration with nine 150 µL samples, each containing 1 µM enzyme and a substrate (pNPP) concentration between 0 and 80 mM in reaction buffer. 50 µL of 5 N NaOH was added to end each reaction. The 200 µL samples had to be diluted five-fold to 1mL in order to accurately read with the SpectroVis. We read the absorbances of each sample with the SpectroVis at 405.4 nm, adjusted for the dilution, then converted those values to pNP concentration using the standard curve. We then calculated the rate of reaction for each substrate concentration, and fit the data to the Michaelis Menten equation (Equation 2) to obtain the K_m, k_{cat}, and V_{max} values.

Equation 2

$$V_0 = \frac{V_{max}[S]}{K_m+[S]} = \frac{k_{cat}[E_T][S]}{K_m+[S]}$$

Testing Substrate Affinity

To create a standard curve of phosphate concentration versus absorbance, we created seven samples of 50 µL of $NaPO_4$ concentrations between 0 and 35µM in water. 100 µL of Biomol Green was added to each sample, and after 20 minutes the samples were read at 640 nm. The results were used to create the phosphate standard curve. We then ran an assay of 24 different substrates, with corresponding controls, each with 50 µL of solution that was 0.1 µM enzyme and 100 µM of a different substrate in reaction buffer. We ran each reaction for 15 minutes in a 30ºC incubator, adding 100 µL of Biomol green to stop each reaction. Using the standard curve, we converted the absorbance values to phosphate concentration, with which we could calculate the rate of reaction. With Equation 2, where the [S] is negligible in the denominator because the substrate concentration was low, we calculated the catalytic efficiency of each substrate with *M. oryzae* Cdc14.

Enzyme Modeling & Testing Inhibitor Affinity in silico

In the program Molecular Operating Environment, we created a homology model with the *M. oryzae* Cdc14 sequence and its yeast homolog 5XW5. After it was aligned and the active site identified via superposition with the known crystal structure, 16 inhibitors were docked into the active site and the best conformations, and best bond affinities, were recorded based on lowest S-value.

Testing Inhibitor Affinity in vitro

To calculate the Z-factor of our inhibitor assays, we ran a positive control with 1.6 μM enzyme and 7.2 mM pNPP, and a negative control with no enzyme and 7.2 mM pNPP, both in reaction buffer. We allowed each reaction to commence in a 30℃ incubator for 15 minutes before stopping them with 25 μL of 5N NaOH. We then read the absorbances at 405 nm in a plate reader. To test the affinity of each inhibitor for our enzyme, we ran an assay of 16 different inhibitors, each with 50 μL of solution containing 1 μM enzyme, 7.2 mM pNPP, and 100 μM of chosen inhibitor in reaction buffer. We ran each reaction and read the resulting absorbances under the same conditions as the Z-factor assay. This assay was performed in triplicate with controls. Assays to obtain the IC_{50} were performed with the three inhibitors that showed the greatest affinity and were available, I1, I2, and G5. For each inhibitor, we ran an assay at 13 different inhibitor concentrations;13 two-fold dilutions starting at 500μL. Each sample also contained 1 μM enzyme and 7.2 mM substrate in a 100 μL total solution. We ran each reaction for 15 minutes at 30 C^o and stopped each one with 25 μL of 5N NaOH. We read the samples in a plate reader at 405 nm. The percent activity was calculated for each inhibitor by scaling the greatest absorbance to 100% activity and the least absorbance to 0%, and graphed to fit equation 3.

Equation 3

$$\%\ activity = \frac{100}{1+10^{(log[inhibitor]-log[IC50])\cdot B}}$$

In Equation 3, B represented an adjustment constant, and log[inhibitor] was the x-axis variable. The IC_{50} was obtained with this curve fit in Logger Pro.

I2 Reversibility Testing

Two reversibility assays with 10 reactions each were performed with the I2 inhibitor. Microfuge tubes of 80μL of 1μM enzyme and 3μM I2 in reaction buffer were pre-incubated for select amounts of time between 0 and 60 minutes. Then pNPP was added to achieve a concentration of 7.2mM for each tube and the reaction was run for 15 minutes at 30 C^o. 45μL of 5N NaOH was added after those 15 minutes to stop the reaction and bring the final volume to 125μL. The absorbance value of each solution was read in a plate reader at 405 nm and used to calculate percent activity for each pre-incubation time.

Designing Greater Affinity Inhibition

After aligning I2 as a ligand to the homology model, we made note of the docking score and the ligand efficiency. We then modified the ligand by adding a trifluoromethyl group to the original carbon chain of I2. In addition, two carbon chains containing multiple benzene rings and carbonyl groups were added to the original ring, replacing two hydroxyl groups. An additional trifluoromethyl group was also added to one of the additional new chains. These additions were made to mimic the real substrate and conform to the binding pocket of the enzyme. The conformational energy was minimized in MOE after each modification. We recorded each change and the corresponding docking score.

Acknowledgements

We thank Dr. Mark Hall, Dr. Martha Oakley, Hannah Nikole Almonte, Jake Crosser, Emily Overway, Devin Srivastava, and John Whitney for their guidance throughout this project. We also thank Purdue for hosting us and our research.

Correspondence
Kaitlyn Crowley: kc774786@gmail.com
Hyowon(Raphi)Kang:
h.raphaela.kang@gmail.com
Alan Tondryk: alantondryk@gmail.com

Figures and Tables

A

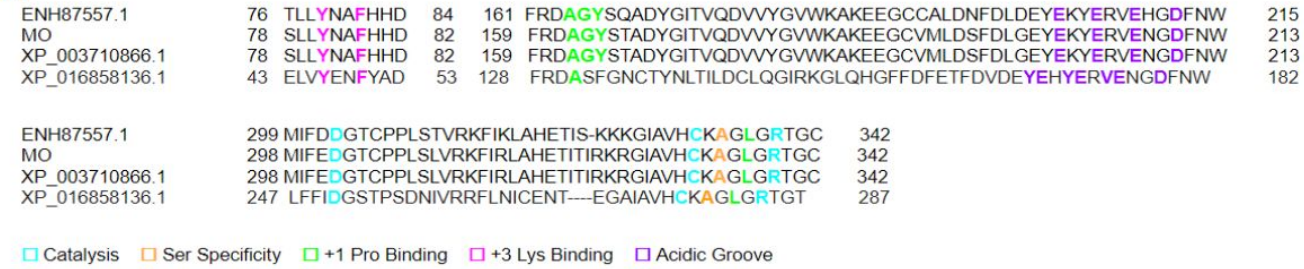

B

	No sodium orthovanadate specific activity (min^{-1})	With sodium orthovanadate specific activity (min^{-1})
Average	5.96	4.01
Standard Deviation	0.01	0.37

Figure 1. Specific activity and binding site sequence of *M. oryzae* Cdc14 reveals enzyme specificity.
A. Alignment of the *CHomo sapian* Cdc14 sequence (XP_016858136.1), our Cdc14 sequence (MO), and the M.O. Cdc14 sequence (XP_003710866.1) which had a 100% identity with the query sequence on blast reveals the conservation of the Cdc14 active site sequence in all three sequences. Similar features show conserved, thereby functional, regions. The amino acid residues crucial for specificity are colored according to their function in the diagram.

B. The specific activity of *M. oryzae* Cdc14 with pNPP (p-Nitrophenyl Phosphate) with and without the presence of sodium orthovanadate was calculated as an average of three trials. pNPP is a substrate that contains a phosphate group, and sodium orthovanadate is a competitive inhibitor for phosphatases.

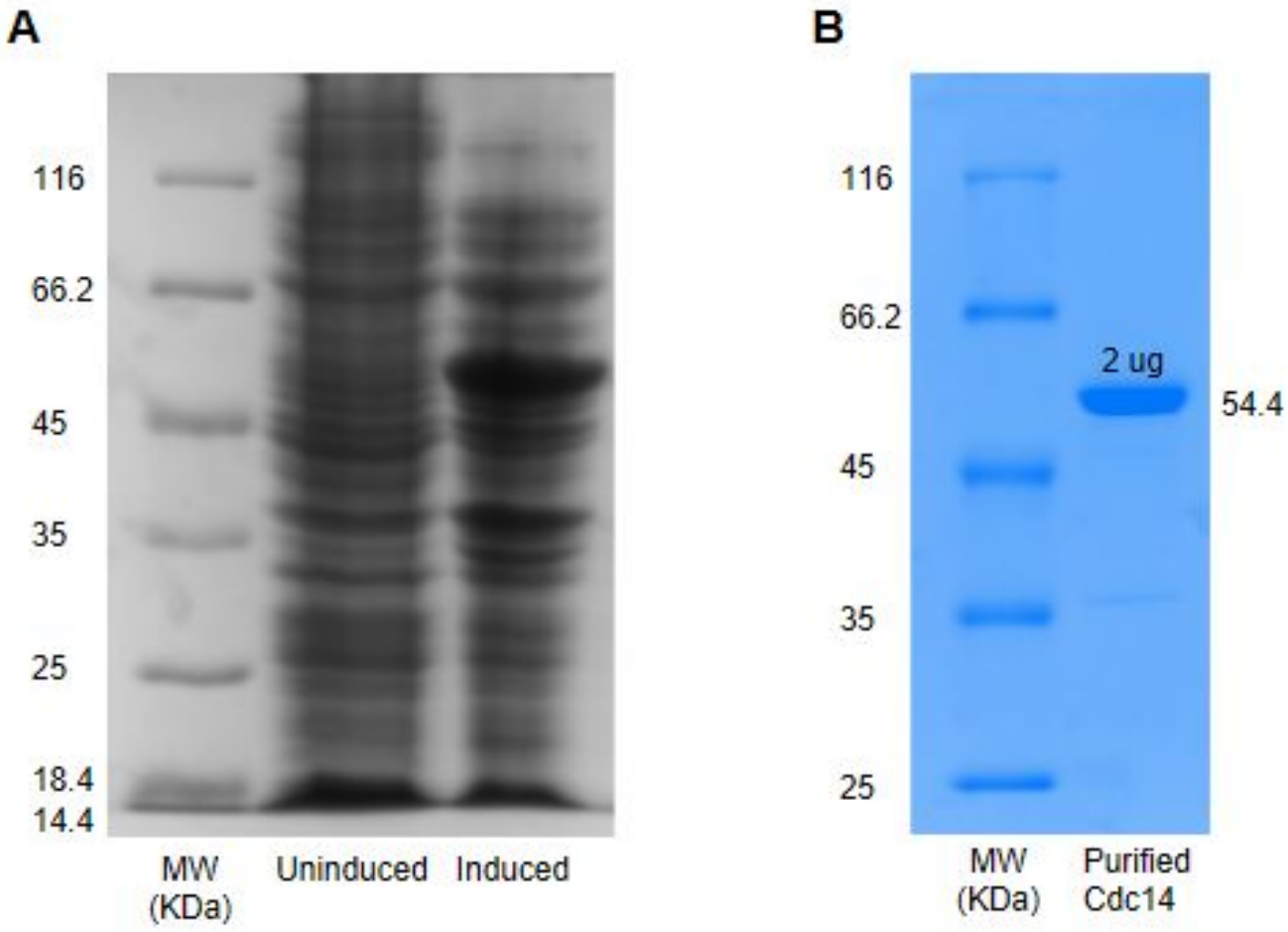

Figure 2. Expression and purification gels show expressed and purified Cdc14.

A. Both samples have many bands present, however while the induced sample has many of the same bands, it has a darker band between 45 and 66.2 KDa.

B. The rightmost band represents how far the protein sample travelled in a polyacrylamide gel over one hour at a voltage of 180V. The thickest band represents our protein at 1.959μM with a molecular weight of 54.4 KDa, which is further shown by the molecular weight marker bands. The concentration of the purified protein, 500 ng, was determined by comparing it to the BSA standards.

A

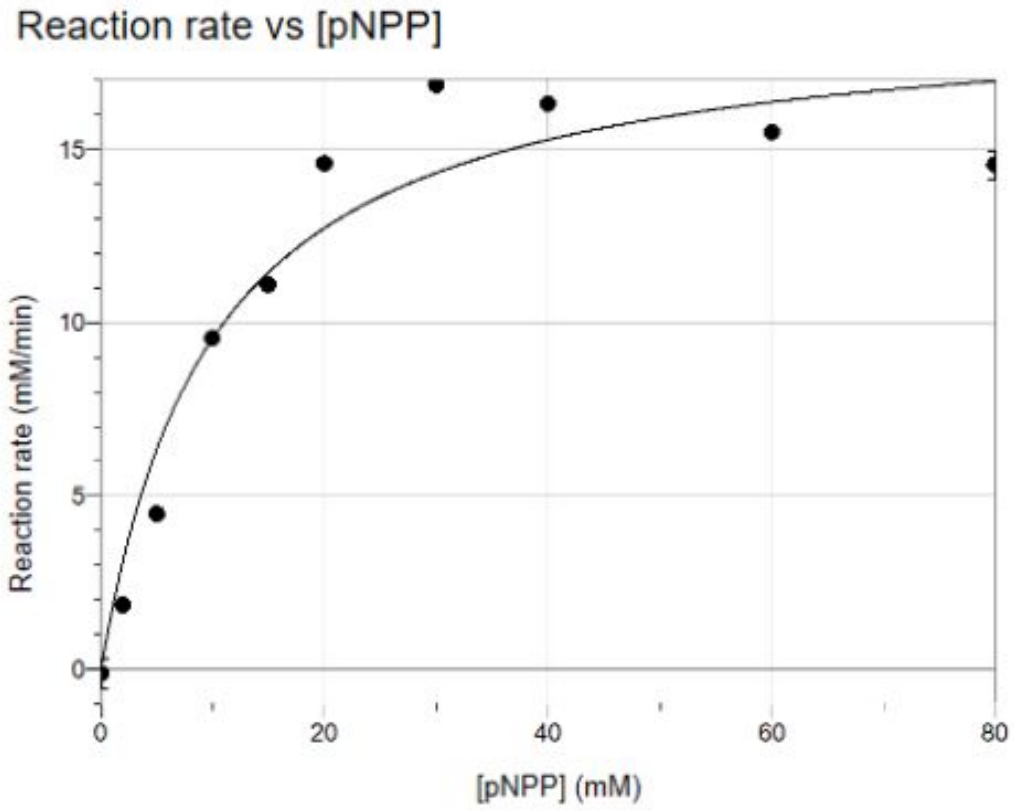

B

	V_{max} (mM/min)	k_{cat} (min^{-1})	K_m (mM)
Average	17.72	17.58	9.12
Standard Deviation	2.44	2.48	2.26

Figure 3. pNPP Michaelis-Menten curve is used for determining kinetic properties.
A. Each data point is an average of three trials, representing the rate of reaction at each pNPP concentration. From this graph we can calculate the V_{max}, k_{cat}, and K_m values for pNPP and *M. oryzae* Cdc14. The RMSE value is 1.701.
B. Cdc14 enzyme kinetic properties are determined from the Michaelis-Menten curve.

A

Substrate	Sequence
1	HT{pS}PIKSIG
2	HT{pT}PIKSIG
3	HT{pY}PIKSIG
4	HT{pS}AIKSIG
5	HT{pS}PIASIG
6	HT{pS}PIRSIG
7	HT{pS}PIKKIG
8	HT{pS}PKKSIG
9	HT{pS}PIKSKG
10	HT{pS}PKASIG
11	HT{pS}PIAKIG
12	HT{pS}PIASKG
13	HT{pS}PIASIK
14	AT{pS}PIKSIG
15	HA{pS}PIKSIG
16	HT{pS}KIKSIG
17	HT{pS}PEKSIG
18	HT{pS}PIKEIG
19	HT{pS}PIKSEG
20	HT{pS}PIKSIE
21	HT{pS}PIKSIK
22	KT{pS}PIKSIG
23	HK{pS}PIKSIG
24	HT{pS}PIKKRG

B

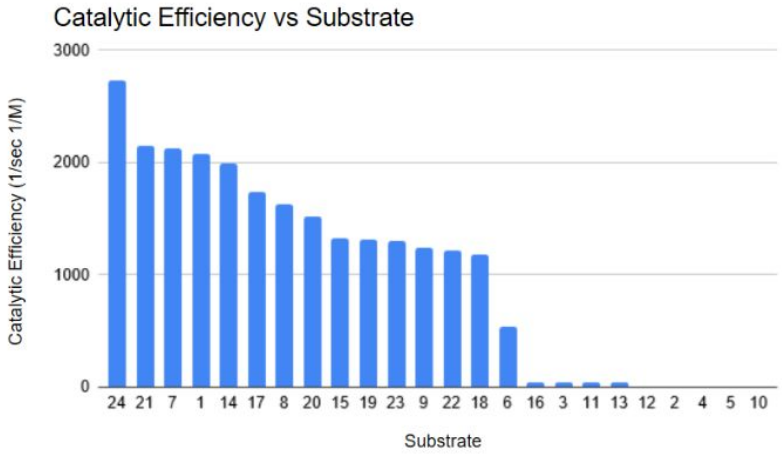

Figure 4. Most effective substrates based on catalytic efficiency.

A. The sequence of the 24 tested substrates is shown above; their amino acid sequence determines the level of their interaction with the catalytic site on *M. oryzae* Cdc14.

B. The figure illustrates the k_{cat}/K_m (catalytic efficiency) value of each substrate, measured in units of $sec^{-1}M^{-1}$. The most effective substrate for our target protein was 24, which had a catalytic efficiency of 2737 $sec^{-1}M^{-1}$.

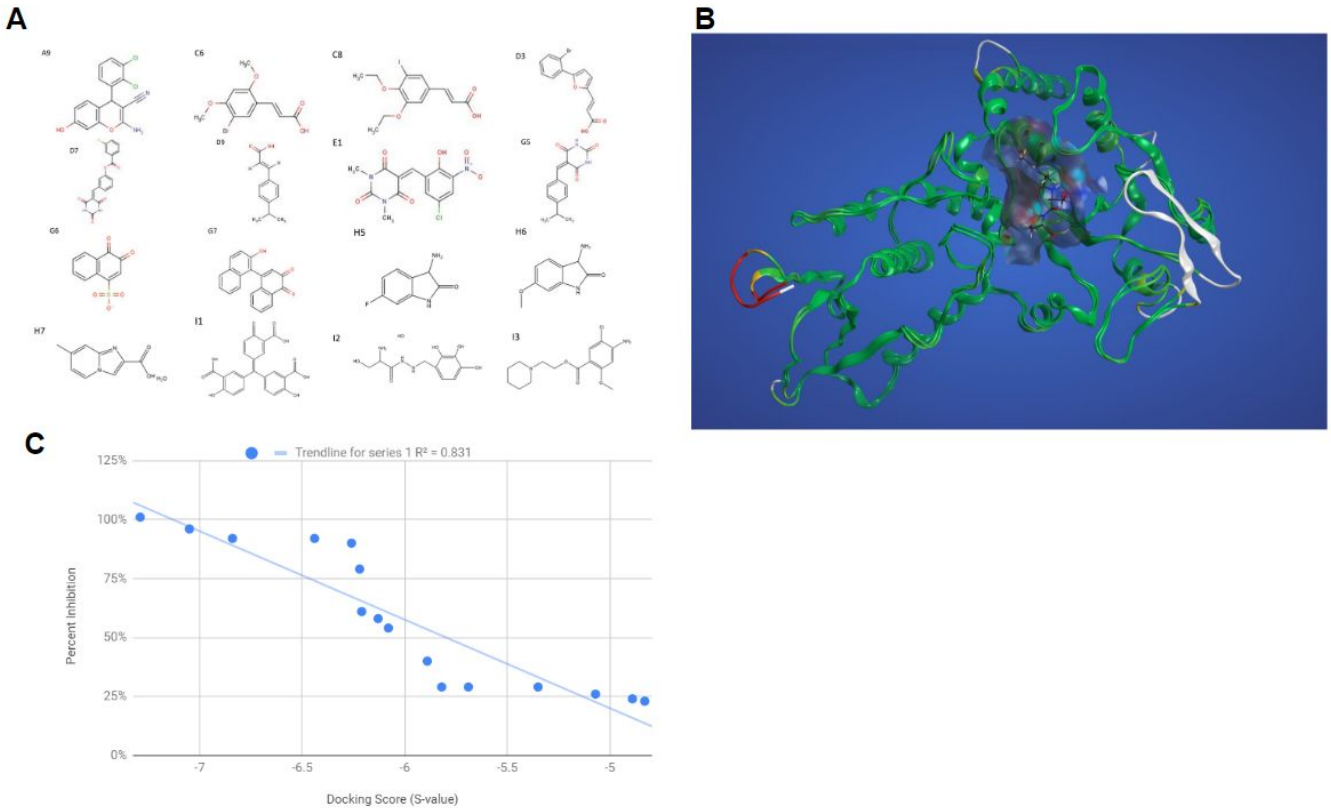

Figure 5. Most effective inhibitors based on in vitro experiments.

A. The structure of all 16 tested inhibitors is shown.

B. The green regions around the catalytic site represent conserved regions between the homology model and the yeast Cdc14. The white, orange, and red regions are the non conserved regions. This model was used to dock and test inhibitors in silico.

C. The percent inhibition was graphed based on docking score in kcal/mol. A correlation (R^2 value) of 0.831 was observed.

Substrate	S-value	Percent Inhibition
I1	-7.29	92%
E1	-7.05	79%
D7	-6.84	58%
A9	-6.44	26%
I2	-6.26	90%
C8	-6.22	29%
G7	-6.21	101%
G5	-6.13	92%
I3	-6.08	29%
C6	-5.89	29%
G6	-5.82	96%
D3	-5.69	40%
D9	-5.35	24%
H6	-5.07	23%
H7	-4.89	54%
H5	-4.83	61%

Table 1. Experimentally determined inhibitor activity.

The MOE docking results showed that inhibitors I1, E1, and D7 should be the most effective, based on their S-values(in kcal/mol). The S-value indicates the binding free energy of the conformation; so a greater negative S-value indicates a greater inhibitor affinity. This is based on the results of inhibitor docking with the homology model.

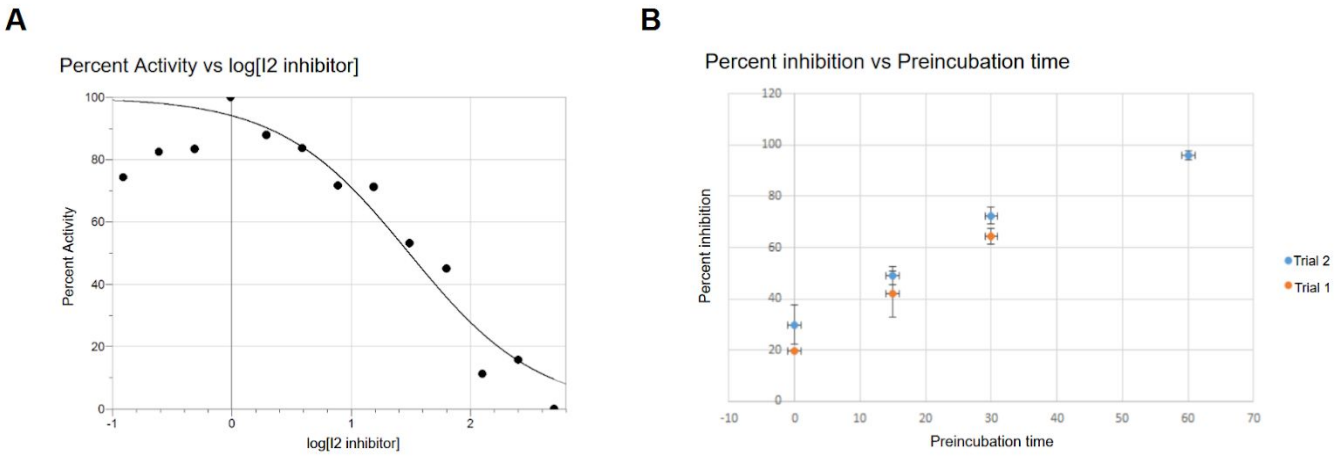

Figure 6. I2 binding mechanism and IC_{50} for *M. oryzae* Cdc14.

A. I2 had an IC_{50} value of 31.9μM. The RMSE value for this curve fit was 11.63. Our Z-factor for this assay was 0.62.

B. This graph was based on two trials of a reversibility assay using the I2 inhibitor. The observable correlation between the percent inhibition and the preincubation time suggests that the I2 inhibitor binds irreversibly to the Cdc14 enzyme of *M. oryzae*. The error bars represent standard deviation, where each data point is the average of three trials. Trial 1 lacks a data point with a 60 minute preincubation time because the reaction was stopped prematurely during experimentation

A

	Binding Affinity (kcal/mol)
I2	-7.66
Modified Inhibitor	-16.56

B

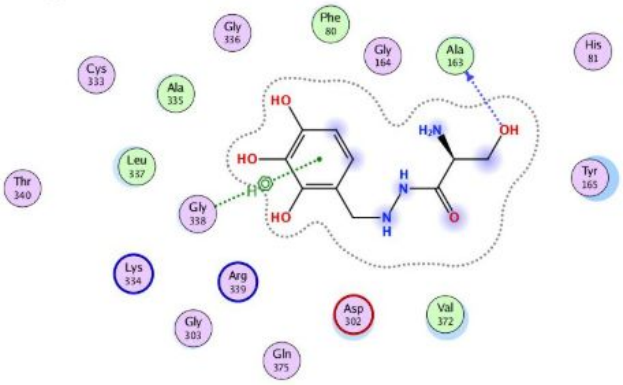

I2 Structure

C

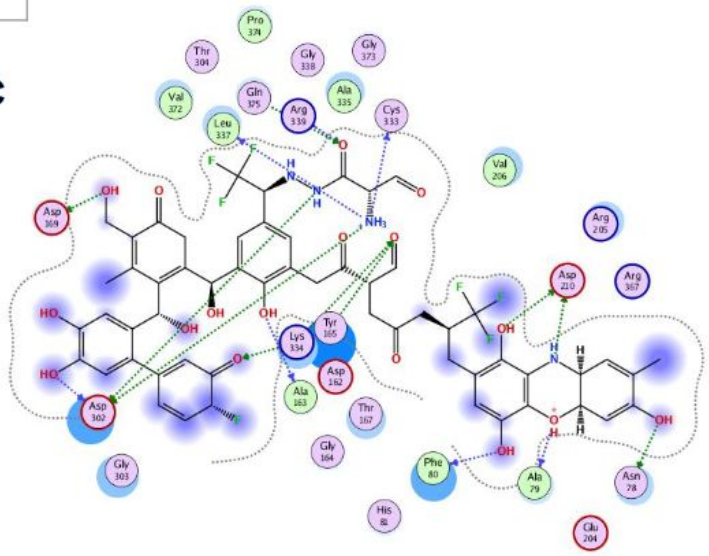

Modified Inhibitor Structure

Figure 7. Modified I2 displays greater affinity for *M. oryzae* Cdc14 active site.

A. The change in structure of I2 and the modified inhibitor increased the binding affinity.

B. The I2 ligand interaction map shows the interactions between the amino acid residues at the binding site and the docked ligand. The green amino acids are greasy, the pink polar. The red rings indicate acidity, the blue basicness, and the green arrows indicate a sidechain H-bond donation and the blue arrows a backbone H-bond donation.

C. The modified inhibitor ligand interaction map shows the newly formed interactions between the active site residues and the inhibitor.

References

1. Garwood, P. (2017, September 15). World hunger again on the rise, driven by conflict and climate change, new UN report says. Retrieved July 14, 2018, from http://www.who.int/news-room/detail/15-09-2017-world-hunger-again-on-the-rise-driven-by-conflict-and-climate-change-new-un-report-says
2. Nalley, L., Tsiboe, F., Durand-Morat, A., Shew, A., & Thoma, G. (2016). Economic and Environmental Impact of Rice Blast Pathogen (Magnaporthe oryzae) Alleviation in the United States. *Plos One, 11*(12). doi:10.1371/journal.pone.0167295
3. Maria S. (2014). Rice Blast: Understanding the Threat. *Pathway Studio, Plant.* https://www.elsevier.com/__data/assets/pdf_file/0008/96983/rice-blast-understanding-the-threat.pdf (Accessed July 22, 2018)
4. Mocciaro, A., & Schiebel, E. (2010). Cdc14: A highly conserved family of phosphatases with non-conserved functions? *Journal of Cell Science, 123*(17), 2867-2876. doi:10.1242/jcs.074815
5. Amon, A. (2008). A decade of Cdc14 - a personal perspective Delivered on 9 July 2007 at the 32nd FEBS Congress in Vienna, Austria. *FEBS Journal, 275*(23), 5774-5784. doi:10.1111/j.1742-4658.2008.06693.x
6. Powers, B. L., & Hall, M. C. (2017). Re-examining the role of Cdc14 phosphatase in reversal of Cdk phosphorylation during mitotic exit. *Journal of Cell Science, 130*(16), 2673-2681. doi:10.1242/jcs.201012
7. Dulev, S., Renty, C. D., Mehta, R., Minkov, I., Schwob, E., & Strunnikov, A. (2009). Essential global role of Cdc14 in DNA synthesis revealed by chromosome underreplication unrecognized by checkpoints in cdc14 mutants. *Proceedings of the National Academy of Sciences, 106*(34), 14466-14471. doi:10.1073/pnas.0900190106
8. Yang, G., Hu, Y., Fasoyin, O. E., Yue, Y., Chen, L., Qiu, Y., . . . Wang, S. (2018). The Aspergillus flavus Phosphatase Cdc14 Regulates Development, Aflatoxin Biosynthesis and Pathogenicity. *Frontiers in Cellular and Infection Microbiology*, 8. doi:10.3389/fcimb.2018.00141
9. Li, C., Melesse, M., Zhang, S., Hao, C., Wang, C., Zhang, H., . . . Xu, J. (2015). FgCdc14 regulates cytokinesis, morphogenesis, and pathogenesis in Fusarium graminearum. *Molecular Microbiology, 98*(4), 770-786. doi:10.1111/mmi.13157
10. Bremmer, S. C., Hall, H., Martinez, J. S., Eissler, C. L., Hinrichsen, T. H., Rossie, S., . . . Charbonneau, H. (2011). Cdc14 Phosphatases Preferentially Dephosphorylate a Subset of Cyclin-dependent kinase (Cdk) Sites Containing Phosphoserine. *Journal of Biological Chemistry, 287*(3), 1662-1669. doi:10.1074/jbc.m111.281105